ELSEVIER

Carbohydrate Research 259 (1994) 175–190

CARBOHYDRATE RESEARCH

Synthesis and conformational analysis of 2-(indol-3-yl)ethyl α-L-arabinopyranoside and its 2,3,4-tri-O-acetyl derivative

Sanja Tomić [a], Bouke P. van Eijck [b], Jan Kroon [b], Biserka Kojić-Prodić [a,*], Goran Laćan [a], Volker Magnus [a], Helmut Duddeck [c], Monika Hiegemann [d]

[a] *Rudjer Bošković Institute, P.O.B. 1016, 41001 Zagreb, Croatia*
[b] *Department of Crystal and Structural Chemistry, Bijvoet Center for Biomolecular Research, Rijksuniversiteit Utrecht, Padualaan 8, 3584 CH Utrecht, Netherlands*
[c] *Universität Hannover, Institut für Organische Chemie, Schneiderberg 1B, D-30167 Hannover, Germany*
[d] *Ruhr-Universität Bochum, Lehrstuhl für Strukturchemie, Postfach 10 21 48, D-44780 Bochum, Germany*

(Received July 20th, 1993; accepted January 8th, 1994)

Abstract

2-(Indol-3-yl)ethyl α-L-arabinopyranoside (**5**) was prepared by Königs–Knorr condensation of the aglycon alcohol with 2,3,4-*O*-acetyl-β-L-arabinopyranosyl bromide, followed by *O*-deacetylation. The structure of the per-*O*-acetylated derivative (**3**) was determined. The crystals of **3** are trigonal, space group $P3_121$ with $a = 8.367(4)$ Å, $c = 53.34(2)$ Å, and $Z = 6$. The conformational analysis is based on the results obtained from X-ray structure analysis (**3**), $^1H\{^1H\}$NOE measurements (**3**), and such computational chemistry methods as molecular mechanics and molecular dynamics simulations (**5**). The α-L-arabinopyranose ring is in a $^4C_1$ chair. Theoretical conformational analysis has been focused on the most flexible part of the molecule defined by four torsion angles about bonds which connect the carbohydrate residue and the indole nucleus. The conformer observed in the solid state is one of several possible forms indicated by molecular mechanics and molecular dynamics. The most probable forms are identified. In all observed conformers, the molecule studied maintains the indole ring approximately perpendicular to the side chain, which may be one of the prerequisites for bioactivity.

1. Introduction

Our structural studies of biologically active, ring-substitued derivatives [1] and amino acid conjugates [2,3] of the plant hormone auxin, indole-3-acetic acid (IAA),

* Corresponding author.

0008-6215/94/$07.00 © 1994 Elsevier Science B.V. All rights reserved
SSDI 0008-6215(94)00040-M

aroused our interest in a further group of compounds of outstanding importance in auxin biochemistry, the glycosides [4]. In this paper, we describe the synthesis, X-ray structure analysis, NMR spectroscopy ($^1H\{^1H\}$NOE measurements), as well as molecular mechanics and dynamics of carbohydrate conjugates of 2-(indol-3-yl)ethanol (tryptophol).

The alcohol is an endogenous plant constituent [5] which appears to be in an oxidase–reductase-mediated equilibrium with the IAA precursor, indole-3-acetaldehyde. The oxidase has been isolated and found to be feed-back inhibited by IAA [6]. This points to the involvement of tryptophol in the stabilisation of auxin levels in plants, and reversible conjugation of the alcohol would enhance the capacity of such a buffer mechanism. While the endogenous tryptophol conjugates [5] have not been completely identified, exogenously applied tryptophol is metabolised by bacteria, thallophytes, and seed plants, to esters and glycosides: the β-D-glucopyranoside (most cases) and/or the β-D-galactopyranoside (some unicellular algae) [7,8]. Tryptophol glycosides can apparently be reutilised for IAA biosynthesis since the β-D-glucopyranoside [9] and, in particular, the α-L-arabinopyranoside [8] support growth and differentiation in a plant tissue culture system which can develop only if a source of auxin is supplied in the nutrient medium [10]. 2-(Indol-3-yl)ethyl α-L-arabinopyranoside was therefore chosen as a subject of this study, with further regard to the fact that this compound represents a class of carbohydrate derivatives which have so far been poorly characterised in structural terms. The Cambridge Structural Database (version 5, 1992) [11] contains only one structure with an α-L-arabinose moiety in its pyranose form [12].

Our strategy was to use the chemically more stable and easily crystallisable per-*O*-acetylated glycoside for X-ray analysis * and NMR measurements, and to derive the structure of the unsubstituted glycoside by computational methods.

Saccharides in plants, particularly in the cell wall, have been shown to be of biological importance [13]. The enzymes associated with the process of cell wall loosening and elongation and their activity have been observed to increase during auxin-stimulated growth [14].

2. Results and discussion

Synthesis.—Condensation of 2,3,4-tri-*O*-acetyl-β-L-arabinopyranosyl bromide (**1**) with a ca. 20% molar excess of 2-(indol-3-yl)ethanol (**2**), in the presence of silver oxide and anhydrous calcium sulfate, afforded the per-*O*-acetylated α-L-arabinopyranoside (**3**) along with the isomeric (*exo*- and *endo*-stereomers) β-L-arabinopyranose 1,2-orthoacetates (**4**).

* Note: The atom numbering of the sugar moiety used in the Experimental section is in agreement with carbohydrate nomenclature. However, in the X-ray analysis and computational chemistry, an additional digit, namely 1, was used in order to be consistent with the indole numbering employed for the auxin series (e.g., O-5 → O-15).

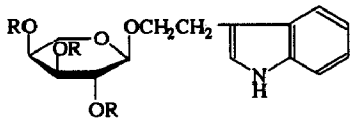

3 R = OAc

5 R = H

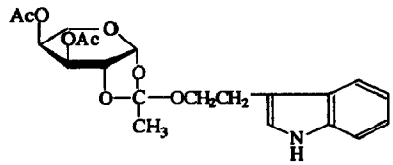

4

The course of the reaction was solvent dependent; the proportions of products **3** and **4** obtained in dichloromethane–diethyl ether solutions are presented in Table 1. Likewise, under identical conditions, condensation of halide **1** with aliphatic and aralkyl alcohols afforded mixtures of the respective glycosides and ortho esters, and this could be rationalised by interaction of ionic intermediates with the solvent ether [5]. This is insufficient to explain the data in Table 1, since ortho ester **4** was also formed in reactions conducted in pure dichloromethane. The dissociation constants for the protonation of indole ($pK_a = -3.5$) and 3-methylindole ($pK_a = -4.55$) [16] indicate, however, that the indole moiety of **2** is about as basic as diethyl ether ($pK_a = -3.59$) [17] and should thus interact with the ionic intermediates in a similar way. In fact, unsubstituted indole reacted with glycosyl halide **1** in boiling benzene containing silver oxide to yield *N*- and *C*-linked condensation products, the per-*O*-acetylated 1- and 3-α-L-arabinopyranosylindoles, and 1,2-*O*-[1-(indol-1-yl)ethylidene]-β-L-arabinopyranose [18]. Formation of analogous products from the indolic alcohol **2** was not observed under the conditions used in our work. Interestingly, 0.1–10% (depending on the solvent composition) of glycosyl halide **1** was reisolated following condensation with **2**. Minor products included up to 3% of 3-(2-acetoxyethyl)indole formed presumably via the ortho ester **4** [19,20]. *O*-Deacetylation of **3** with saturated methanolic ammonia afforded the unprotected arabi-

Table 1
Ratios of per-*O*-acetylated β-L-arabinopyranose, 1,2-orthoacetates (**4**) and α-L-arabinopyranoside (**3**) formed by condensation of glycosyl halide **1** with 2-(indol-3-yl)ethanol (**2**) in dichloromethane–diethyl ether [a]

Ratio of dichloromethane: diethyl ether	Yield[b] (%) of 4+3	Ratio of 4:3
100:0	89	24:76
95:5	89	29:71
85:15	90	30:70
75:25	85	30:70
65:35	81	29:71
50:50	85	27:73
38:62	84	23:77
25:75	68	20:80
0:100	50	0:100

[a] Glycosyl halide **1** (1.1 mmol) and alcohol **2** (1.3 mmol) were reacted under identical conditions (see Experimental for details). [b] Based on **1**.

noside **5**. Both **3** and **5** were crystalline, but only the former yielded crystals suitable for X-ray diffraction analysis.

X-ray structure analysis of **3**.—The structure of **3** with atom numbering is shown in Fig. 1. The ORTEP plot [21] is drawn with thermal ellipsoids at a 30% probability level. Bond lengths and angles are listed in Table 2. The endocyclic bonds O–C [O-15–C-11, 1.419(3) Å; O-15–C-15, 1.435(2) Å] are asymmetrical. The equatorially disposed C-11–O-11 bond [1.378(2) Å] is significantly shorter than a normal C–O bond (1.428 Å), as is usually found for the anomeric C–O bond in equatorial glycopyranosides [22]. The endocyclic angle C-11–O-15–C-15 [111.8(2)°] is smaller than in β-L-arabinose (112.7°) [23] and β-DL-arabinose (113.5°) [24]. The valence angle at the glycosidic oxygen is enlarged to 115.6(2)°. The geometry of the benzene part of the indole nucleus deviates significantly from that of a regular six-membered aromatic ring. Shortening of the C-6–C-7 bond [1.369(5) Å] and shrinkage of the C-6–C-7–C-71 angle [117.0(3)°] were observed in the title compound and in many indole-3-acetic acid derivatives [6] and its amino acid conjugates [5,7].

The overall molecular conformation is described by selected torsion angles presented in Table 3. According to these values and Cremer and Pople [25] parameters [$\theta = 3.0(2)°$; $\varphi = 40(4)°$; $Q = 0.569(2)$ Å], the pyranoid ring is in its $^4C_1$ chair conformation while its orientation with respect to the indole nucleus is determined by the torsion angles about the C-3 → C-11 backbone, i.e., D1(O-15–C-11–O-11–C-9), D2(C-11–O-11–C-9–C-8), D3(O-11–C-9–C-8–C-3), and D4(C-9–C-8–C-3–C-2). The angle D4 between the indole ring plane and the side chain is −115.9(3)°. The conformation about the glycosidic bond is (−) antiperiplanar [D2 = −166.9(2)°] [26]; those about C-11–O-11 and C-9–C-8 (D1 and D3) are synclinal (Table 3).

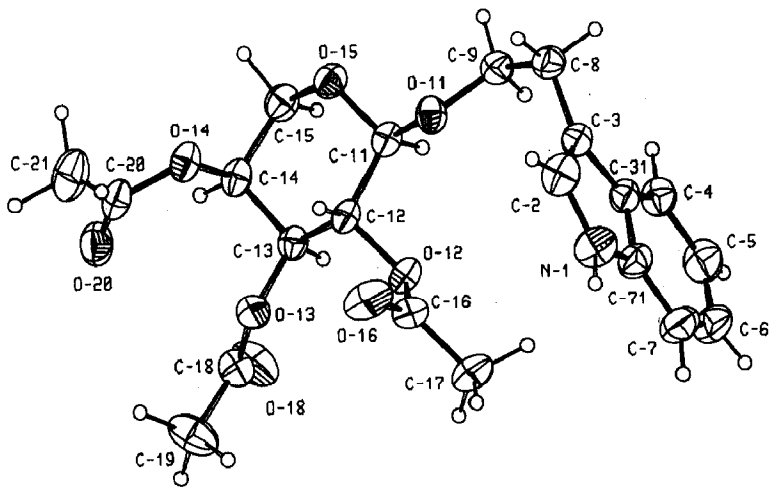

Fig. 1. Molecular structure (ORTEP drawing) of **3** with atom numbering. The thermal ellipsoids are at a 30% probability level.

Table 2
Bond lengths (Å) and angles (°) for 3

Bond length		Bond angle	
Pyranose moiety			
C-11–C-12	1.518(4)	C-11–O-15–C-15	111.8(2)
C-11–O-11	1.378(2)	O-15–C-11–C-12	109.9(2)
C-11–O-15	1.419(3)	C-11–C-12–C-13	109.7(2)
C-12–C-13	1.514(2)	C-12–C-13–C-14	111.0(2)
C-12–C-12	1.433(3)	C-13–C-14–C-15	109.5(2)
C-13–C-14	1.513(3)	O-15–C-15–C-14	111.7(2)
C-13–O-13	1.446(3)		
C-14–O-15	1.516(4)		
C-14–O-14	1.448(3)		
C-15–O-15	1.435(2)		
		C-9–O-11–C-11	115.6(2)
O-12–C-16	1.348(2)	O-11–C-11–C-12	108.3(2)
C-16–O-16	1.192(3)	O-15–C-11–O-11	108.6(2)
C-16–C-17	1.489(4)	O-12–C-12–C-11	107.6(2)
O-13–C-18	1.342(3)	O-12–C-12–C-13	107.3(2)
C-18–O-18	1.193(3)	O-13–C-13–C-12	106.6(2)
C-18–C-19	1.488(5)	O-13–C-13–C-14	111.9(2)
O-14–C-20	1.351(3)	O-14–C-14–C-13	109.3(2)
C-20–O-20	1.193(3)	O-14–C-14–C-15	107.6(2)
C-20–C-21	1.495(5)		
Tryptophol moiety			
N-1–C-2	1.361(4)	O-11–C-9–C-8	108.2(2)
N-1–C-71	1.357(4)	N-1–C-2–C-3	110.8(3)
C-2–C-3	1.356(4)	C-2–N-1–C-71	108.9(2)
C-3–C-8	1.490(4)	C-2–C-3–C-8	126.9(3)
C-3–C-31	1.431(4)	C-2–C-3–C-31	105.6(2)
C-31–C-71	1.405(3)	C-3–C-31–C-4	134.2(2)
C-31–C-4	1.397(4)	C-8–C-3–C-31	127.5(2)
C-4–C-5	1.378(5)	C-3–C-31–C-71	107.2(2)
C-5–C-6	1.406(5)	C-5–C-4–C-31	119.0(3)
C-6–C-7	1.369(5)	C-4–C-31–C-71	118.5(2)
C-7–C-71	1.386(4)	C-4–C-5–C-6	120.8(3)
C-8–C-9	1.512(3)	N-1–C-71–C-7	129.5(3)
C-9–O-11	1.424(4)	C-5–C-6–C-7	121.7(3)
		N-1–C-71–C-31	107.4(3)
		C-6–C-7–C-71	117.0(3)
		C-7–C-71–C-31	123.1(3)
		C-3–C-8–C-9	113.5(2)

The crystal packing is solely through van der Waals interactions. The only potential donor group N-1–H of the indole moiety is not involved in hydrogen bonds. The shortest intermolecular contacts are of the C–H $\cdots$ O type between the C-19 methyl group and the O-18 carbonyl oxygen, 3.542(5) Å, and between the indole moiety C-5–H and the anomeric oxygen O11, 3.481(5) Å.

Table 3
Selected torsion angles (°) for 3 [a]

Endocyclic angle	
O-15–C-11–C-12–C-13	58.3(2)
C-11–C-12–C-13–C-14	−54.2(3)
C-12–C-13–C-14–C-15	52.1(3)
C-13–C-14–C-15–O-15	−54.8(3)
C-14–C-15–O-15–C-11	60.9(3)
C-15–O-15–C-11–C-12	−62.0(2)
Exocyclic angle	
C-15–O-15–C-11–O-11	179.7(2)
O-15–C-11–C-12–O-12	174.7(1)
C-11–C-12–C-13–O-13	−176.3(2)
C-12–C-13–C-14–O-14	−65.5(3)
(D1)O-15–C-11–O-11–C-9	−87.3(3)
(D2)C-11–O-11–C-9–C-8	−166.9(2)
Tryptophol moiety	
(D3)O-11–C-9–C-8–C-3	59.7(3)
(D4)C-9–C-8–C-3–C-2	−115.9(3)
C-9–C-8–C-3–C-31	62.2(4)

[a] The torsional angles D1, D2, D3, and D4 are the subject of theoretical calculations.

Molecular mechanics.—Energy minimisations were carried out using the program DISCOVER, version 2.7.0 (Biosym, 1991) [27], with the CVFF force field based on the work of Lifson and Warshell [28] and Haegler et al. [29,30]. As a start, the crystal structure of **3** was optimised (periodic boundaries, cut off 17 Å). The structure remained very close to that determined by X-ray analysis (Fig. 2). All further work was done on the nonacetylated derivative, compound **5**, treated as an isolated molecule. Starting from the crystal structure, the torsional angle D4(C-9–C-8–C-3–C-2) changed from −116° to −75° (Fig. 2) upon optimisation.

The molecule has much conformational freedom because of the various possibilities for the torsion angles D1, D2, D3, and D4 (Scheme 1). To obtain some idea about the extent of the accessible conformational space, energies were calculated

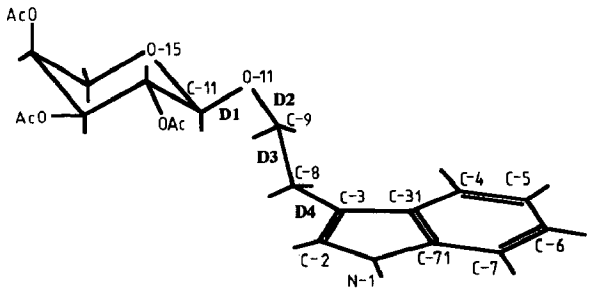

Scheme 1. 2-(Indol)-3-yl)ethyl 2,3,4-tri-*O*-acetyl-α-L-arabinopyranoside with atom numbering and the torsion angle labels.

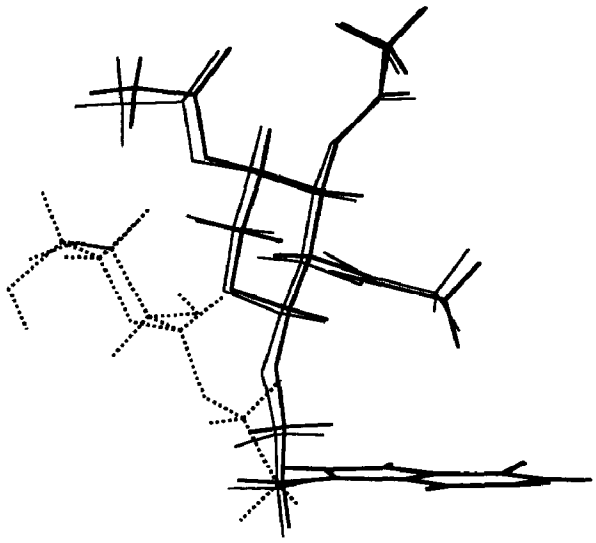

Fig. 2. Overlap of the crystallographically determined conformation (———) of 3, its optimised conformer in the crystal (▬▬), and in vacuo optimised conformer of 5 (------).

for all combinations of these angles in steps of 60°, 36°, 60°, and 90°, respectively. Each calculation was followed by 20 steps of steepest descents minimisation. In this way, promising regions of low potential energy were roughly localised. More detailed information was obtained by making two-dimensional maps in these regions, with the step size reduced to 15° or 10°. Some of these maps are shown in Fig. 3. Finally, full energy minimisation was performed for the lowest minima. As illustrated in Table 4, there are many almost equivalent possibilities.

All the results can be summarised as follows: the conformation about the anomeric bond (D1) is (−)synclinal or (−)anticlinal; about the glycosidic link, a range of conformations is possible with D2 180 ± 75°; for D3, all three staggered conformations occur; and the torsional angle D4 is either +90° or −90°. Thus, the indole plane remains perpendicular to the bond C-8–C-9.

Molecular dynamics.—Molecular dynamics simulations of **5** in aqueous medium at room temperature were also carried out using the DISCOVER program [27]. A water layer of 10 Å (ca. 200 molecules, depending on the starting conformation) was added, and the time step was 1 fs. Fig. 4 shows the evolution of the four angles which determine the conformations, starting from the crystal structure. This structure is now reasonably stable during the short time studied (40 ps). Again a large variability of D1 is encountered.

Other simulations were done from different starting structures. Although it would take an impossibly long time to determine the real equilibrium distribution, some regularities were noticed. The conformation of D1 always ended up as (−)synclinal, and D2 antiperiplanar. The torsional angle D4 was either ca. −90° or +90°. For D3, the conformation was mostly (±)synclinal, but, when D4 was

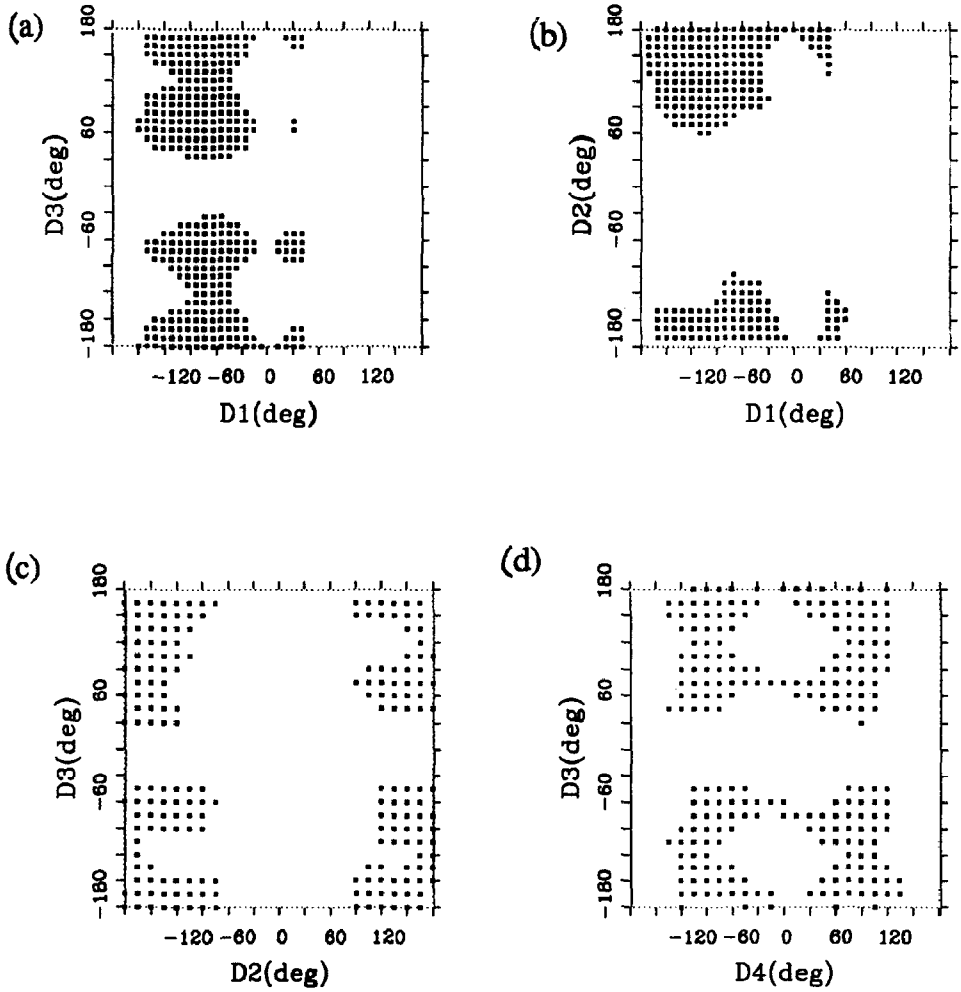

Fig. 3. Two-dimensional energy map for 2-(indol-3-yl)ethyl α-L-arabinopyranoside (**5**) as a function of the two torsion angles: (a) D1 and D3, with D2 ≈ 180°, D4 ≈ 95°; (b) D2 and D1, with D3 ≈ 180°, D4 ≈ 95°; (c) D2 and D3 with D1 ≈ −70°, D4 ≈ 95°; (d) D4 and D3 with D1 ≈ −70°, D2 ≈ 180°; [D1(O-15–C-11–O-11–C-9), D2(C-11–O-11–C-9–C-8), D3 (O-11–C-9–C-8–C-3), D4 (C-2–C-3–C-8–C-9)]. Dots indicate conformations within 5 kcal/mol of the global minimum in the 2D torsion space analysed. The angles are given in degrees (°).

+90°, the antiperiplanar conformation for D3 remained stable during 40 ps of simulation on room temperature.

Alternatively, the GROMOS [31] force field and program package were used for simulations of **5**, surrounded by 250 SPC water molecules [32] in a truncated octahedron with periodic boundary conditions. Bond lengths were kept fixed, the cut-off radius was 9 Å, and the system was loosely coupled to a pressure bath of 1 atm and a temperature bath of 298 K. Now the crystal structure conformation changed after 25 ps into a new form, with all four torsional angles (−)synclinal. To

Table 4
The optimised [a] conformers of **5**

Torsion angles (°) (D1, D2, D3, D4)	ΔE_{conf}(kcal/mol)
−142, −175, 179, 98	1
−150, 172, −70, 78	2
−150, −145, 68, 94	0
−72, 174, −179, −98	1
−147, 100, −72, −86	0
−68, −167, 71, −75	1
−54, −144, 64, −99	1

[a] The optimisation obtained by DISCOVER [27].

explore the configuration space further, simulations were done with the temperatures increased in steps of 50 K up to 750 K. Several conformations were observed; a quenching procedure reduced them to four new forms (Table 5). To make transitions by rotations easier, 40 ps of simulation was performed at 500 K

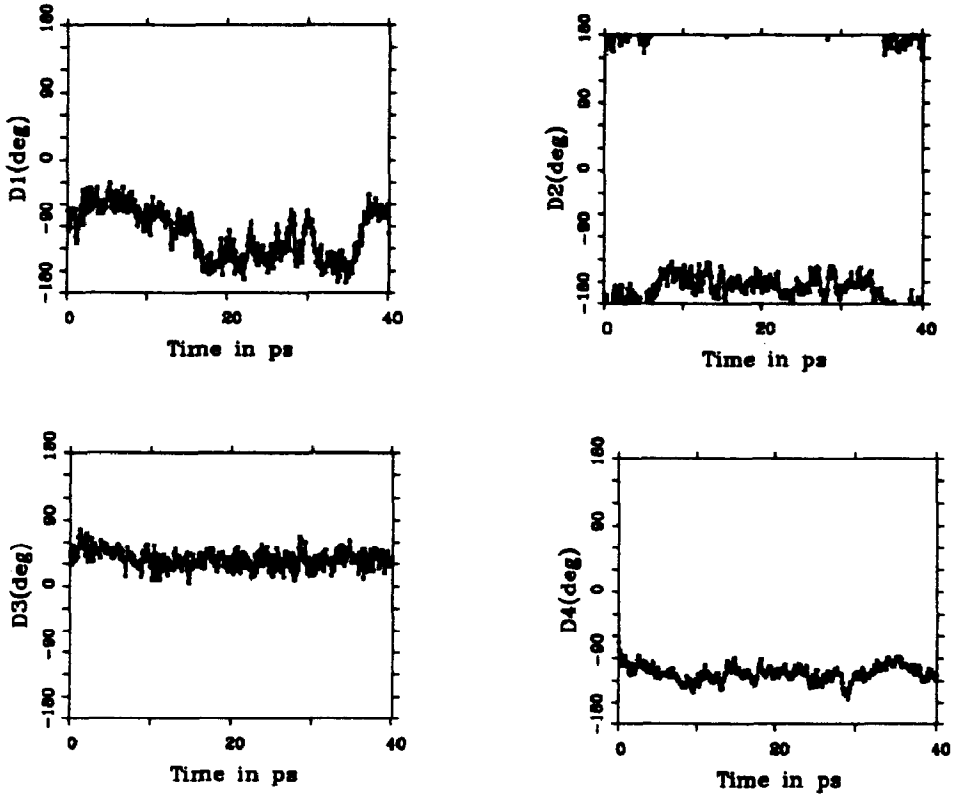

Fig. 4. Variations of torsion angles D1, D2, D3, and D4 of 2-(indol-3-yl)ethyl α-L-arabinopyranoside during MD simulation at room temperature, over 40 ps (DISCOVER), starting from the crystal strucuture [D1 = −87°, D2 = −167°, D3 ≈ 60°, D4 ≈ −117°].

Table 5
Resulting conformations (±30° range) obtained by molecular dynamics simulations of **5** at elevated temperatures up to 750 K, followed by quenching

Torsion angles (°)			
D1	D2	D3	D4
−90	180	180	90
−90	180	−60	−90
60	180	−60	−90
−90	180	60	90

(conformations of rings at that temperature remain stable); Fig. 5 illustrates the variability in torsional angles during the simulation. Although oscillations of D1 (with a mean value ca. −60°) were large, no transitions to (+)synclinal conformation occurred, D2 was mostly ca. 180°, while the conformation of D3 was (−)synclinal for D4 ca. −90°, and (+)synclinal or antiperiplanar for D4 ca. +90°.

In general, the GROMOS results are similar to those obtained by DISCOVER.

Conformation of **3** *in solution*.—In conformationally flexible molecular systems, $^1H\{^1H\}$NOE experiments produce responses for all conformers with reasonable populations [33]. Therefore, in a molecule as mobile as the present — we investigated **3** in $CDCl_3$ at 400.1 MHz (a Bruker AM-400 spectrometer) — a great number of NOEs occur which are not consistent with one single structure. Nevertheless, it was possible to extract some pieces of evidence which confirm the above X-ray and the MD results.

According to our measurements, the two diastereotopic H-9 atoms (H-9a at $\delta = 4.14$ and H-9b at $\delta = 3.75$) are in rather different spatial distances with respect to the anomeric hydrogen H-11. Whereas for one (H-9a), the mutual responses are strong, namely 9.8% (H-9a–H-11) and 9.2% (H-11–H-9a), the corresponding

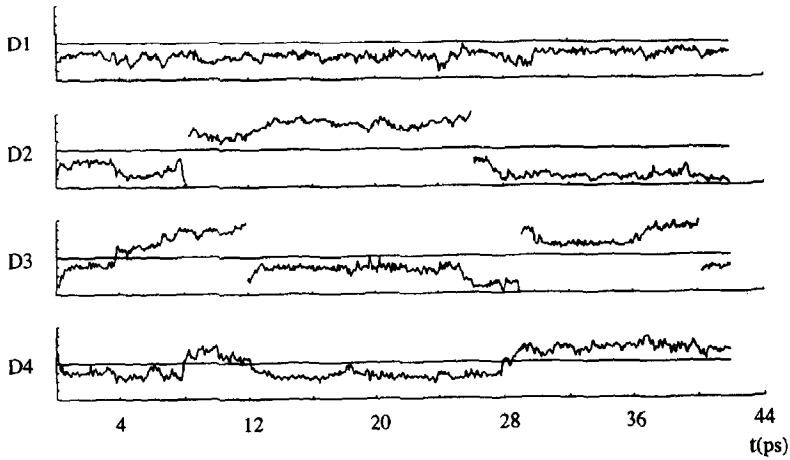

Fig. 5. Variations of torsion angles D1, D2, D3, and D4 of 2-(indol-3-yl)ethyl α-L-arabinopyranoside during MD simulation at high temperature (500 K), over 40 ps (GROMOS).

values for the other (H-9b) are rather small (2.5 and 3.4%, respectively). This supports an antiperiplanar and (−)synclinal orientation about D1. Thus, the stereochemical assignment of the two hydrogens are: H-9a *pro-S* and H-9b *pro-R*.

Only rather small NOE values (1.7 to 4.0%) are observed when the distances between the H-9 atoms and H-2 and H-4 are examined, indicating that there is no preferred conformation with a small distance between any of these pairs. This confirms the MD finding that the indole moiety is more or less perpendicular to the CH_2–CH_2 side chain in both possible directions (D-4 ≈ 90° and −90°).

In addition, there are slight NOEs indicating contacts (but not too close) between the methyl group in the 12-acetate ($\delta = 1.88$) and H-2/H-4. This is consistent with the high flexibility of the side chain around D3, but this requires the acetate group to be positioned predominantly on the β-side of the molecule. Thus, it has to be far away from any of the H-9 atoms and, consequently, no corresponding NOE response at all can be observed.

3. Conclusions

Although an exhaustive conformational search was beyond our possibilities, some tentative conclusions can be drawn. Negative values for D1, the torsional angle about the anomeric bond, were encountered most of the time (Fig. 5, Table 4), although large fluctuations are possible. The torsional angle D2 is mostly found around 180°, again with a large spread. For D3, all three staggered forms occur, whereas the torsional angle D4 is always ca. ±90°. Since this summary covers the results from X-ray analysis, molecular mechanics (DISCOVER), and molecular dynamics (DISCOVER and GROMOS), we believe that it gives an adequate description of the considerable conformational freedom of the molecule.

In the title molecule and many auxin-type compounds, but also in their inactive analogues, the indole moiety is almost perpendicular to the side chain (D4 ≈ 90 ± 25°) as was determined by X-ray structure analysis [2,3]. This is in agreement with the theoretical work reported here, and also with ab initio SCF-MO calculations on indole-3-acetic acid [34]. Here the D4 ≈ 90° conformer was found to be lower in energy by ca. 2 kcal/mol than the conformer with D4 ≈ 0°. Kaethner [35] proposed a mechanism for auxin binding to a receptor where the protein recognises a D4 ≈ 180° conformation which subsequently changes into D4 ≈ 90° during enzymatic reaction. From the present knowledge, there is still no experimental evidence for this hypothesis. A more complete understanding of reaction mechanism would come from kinetic measurements and the X-ray structure determination of a receptor + substrate complex.

4. Experimental

General.—Melting points were determined in open capillaries and are reported uncorrected. Optical rotations were measured with a Zeiss Kreispolarimeter. Routine ^1H NMR spectra were recorded at 100 MHz on a Jeol FX-100 Fourier

transform spectrometer, using Me_4Si as an internal standard. Analytical TLC was performed on Silica Gel GF (Merck) with detection by UV fluorescence and by spraying with 10% H_2SO_4 in EtOH and heating. Preparative chromatography was accomplished by TLC on Silica Gel PF_{254} (Merck) or on a column (65 × 2 cm) containing a mixture of Silica Gel H (65 g) and Celite (40 g) (Kemika, Zagreb, Croatia).

Condensation of 2,3,4-tri-O-acetyl-β-L-arabinosyl bromide (**1**) *with 2-(indol-3-yl)ethanol* (**2**).—Reactions were carried out in the dark, at room temperature, in anhyd CH_2Cl_2–diethyl ether as specified in Table 1. To a stirred solution of **2** (209 mg, 1.3 mmol) in solvent (20 mL) containing anhyd $CaSO_4$ (0.5 g) and dry Ag_2O (0.15 g, 0.65 mmol) was added, in small portions during 1 h, a solution of **1** [36] (373 mg, 1.1 mmol) in the same amount of solvent. The mixture was further stirred for 16 h and then centrifuged. The supernatant solution was concentrated in vacuo and the residue was immediately subjected to column chromatography (elution with 4:1 CH_2Cl_2–diethyl ether) to yield, in this order: (*a*) residual **1**, (*b*) 3-(2-acetoxyethyl)indole, (*c*) ortho ester **4** (*endo*-isomer enriched in first fractions), and (*d*) glycoside **3**. The composition of overlapping fractions was deduced from integrated peak areas in the ^1H NMR spectra. The isolation of more polar components in the crude reaction mixture, such as unreacted **2** and 2,3,4-tri-*O*-acetyl-arabinopyranose (identified by TLC using the same solvent as for column chromatography), was not attempted. Further work-up and characterisation was as follows.

(*a*) 2,3,4-Tri-*O*-acetyl-β-L-arabinopyranosyl bromide (**1**). The following amounts were reisolated following condensation with **2** (solvent in parentheses) and identified by ^1H NMR spectra: 7% (diethyl ether), 2% (25:75 CH_2Cl_2–diethyl ether), 0.1–1% (other solvents listed in Table 1).

(*b*) 3-(2-Acetoxyethyl)indole. Yields varied from 0.2–3% with no obvious dependence on solvent composition. ^1H NMR data ($CDCl_3$): δ 2.06 (s, 3 H, OAc), 3.10 (t, 2 H, *J* 7.3 Hz, ArCH_2), 4.35 (t, 2 H, CH_2O), 8.04 (broad s, 1 H, NH), 7.68–7.07 (m, 5 H, indole CH).

(*c*) 3,4-Di-*O*-acetyl-1,2-*O*-{1-[2-(indol-3-yl)ethoxy]ethylidene}-β-L-arabinopyranose (**4**). The product obtained by column chromatography (*exo*:*endo* ca. 3:1) was purified by preparative TLC, using multiple development with 100:1 CH_2Cl_2–diethyl ether, to yield the title compound as an amorphous white solid. The analytical sample was dried in vacuo at 50° C. ^1H NMR data ($CDCl_3$), *exo* isomer: δ 5.43 (d, 1 H, $J_{1,2}$ 3.9 Hz, H-1), 5.01–5.38 (m, 2 H, H-3,4), 4.12 (m, 1 H, H-2), 4.02 (dd, 1 H, $J_{4,5a}$ 4.5, $J_{5a,5b}$ 12.2 Hz, H-5a), 3.69 (dd, 1 H, $J_{4,5b}$ 4.9 Hz, H-5b), 2.04, 2.08 (2 s, 6 H, 2 OAc), 1.71 (s, 3 H, ethylidene CH_3), 3.03 (t, 2 H, *J* 7.3 Hz, ArCH_2), 3.79 (t, 2 H, CH_2O); *endo* isomer (only intense signals discernible in mixture of isomers): δ 3.05 (t, 2 H, *J* 6.8 Hz, ArCH_2), 2.06, 2.08 (2 s, 6 H, 2 OAc), 1.59 (s, 3 H, ethylidene CH); both isomers: δ 8.06 (broad s, 1 H, NH), 6.90–7.65 (m, 5 H, indole CH). Anal. Calcd for $C_{21}H_{25}NO_8$ (419.42): C, 60.13; H, 6.01; N, 3.34. Found: C, 59.96; H, 5.98; N, 3.05.

(*d*) 2-(Indol-3-yl)ethyl 2,3,4-tri-*O*-acetyl α-L-arabinopyranoside (**3**). Recrystallisation from CH_2Cl_2–hexane afforded colorless prisms; mp 116–118° C; $[\alpha]_D$ +9°

(*c* 0.5, $CHCl_3$); ^1H NMR data ($CDCl_3$): δ 4.43 (d, 1 H, $J_{1,2}$ 7.1 Hz, H-1), 5.24 (dd, 1 H, $J_{2,3}$ 9.4 Hz, H-2), 5.00 (dd, 1 H, $J_{3,4}$ 3.4 Hz, H-3), 5.25 (ddd, 1 H, $J_{4,5a}$ 2.9, $J_{4,5b}$ 1.5 Hz, H-4), 4.03 (dd, 1 H, $J_{5a,5b}$ 13.1 Hz, H-5a), 3.59 (dd, 1 H, H-5b), 1.89, 2.01, 2.12 (3 s, 9 H, 3 OAc), 3.05 (t, 2 H, J_{vic} 6.8 Hz, ArCH_2), 4.16 (dt, 1 H, J_{gem} 9.3 Hz, H-9b), 3.76 (dt, 1 H, H-9a), 2.10 (s, 3 H) and 1.99 (s, 3 H) (13- and 14-acetate methyl), 1.88 (s, 3 H, 12-acetate methyl), 8.33 (broad s, 1 H, NH), 6.73–7.57 (m, 5 H, indole CH). The analytical sample was dried in vacuo at 90° C. Anal. Calcd for $C_{21}H_{25}NO_8$ (419.42): C, 60.13; H, 6.01; N, 3.34. Found: C, 59.84; H, 5.96; N, 3.12.

2-(Indol-3-yl)ethyl α-L-arabinopyranoside (**5**).—A solution of **3** (210 mg, 0.50 mmol) in MeOH (20 mL) presaturated with gaseous NH_3 was left (3 h) at room temperature until TLC (8:2 $CHCl_3$–EtOH) indicated complete deacetylation. Evaporation of the solvent gave syrupy **5** which was purified by preparative TLC (8:2 $CHCl_3$–EtOH; R_f 0.8). The resulting amorphous solid (131 mg, 89%) crystallised on addition of CH_2Cl_2–acetone. Recrystallisation from a slowly evaporating solution in acetone afforded the pure title compound; mp 114–116° C; $[\alpha]_D$ −22.5° (*c* 0.5, 95% EtOH); ^1H NMR data (acetone-d_6–D_2O), sugar moiety: δ 4.34 (d, 1 H, $J_{1,2}$ 6.5 Hz, H-1), 3.61–3.91 (m, 4 H, H-2,3,4,5b), 3.51 (dd, 1 H, $J_{4,5a}$ 3.2, $J_{5a,5b}$ 13.2 Hz, H-5a); 2-(indol-3-yl)ethyl moiety: δ 7.23 (m, 1 H, H-2), 7.59 (m,

Table 6
Crystal data and summary of experimental details for **3**

Molecular formula	$C_{21}H_{25}NO_8$
M_r	419.4
Crystal size (mm)	0.5×0.5×0.3
a (Å)	8.367(4)
c (Å)	53.34(2)
γ (°)	120
V (Å^3)	3235.0(3)
Crystal system	trigonal
Space group	$P3_121$
D_x (gcm^{-3})	1.292
Z	6
μ (cm^{-1})	8.0 (Cu $K\alpha$)
F (000)	1332
T (K)	295(2)
No. of reflections used for cell parameters	25
θ range (°) used for cell parameters	2.0–6.1
θ range for intensity measurement (°)	2.0–75.0
hkl range	(−10,10; −10,10; 0,66)
$\omega/2\theta$ scan	0.79+0.15 tan θ
No. of measured reflections	6488
No. of symmetry independent reflections with $I > 2\sigma(I)$	4148
No. of variables	352
R, w = 1	0.045
S	0.47
Final shift/error	< 0.5
Residual electron density $(\Delta\rho)_{max}$, $(\Delta\rho)_{min}$ (eÅ^{-3})	0.19, −0.25

1 H, H-4), 6.99 (td, 1 H, $J_{5,6}$ 7.0, $J_{5,7}$ 1.7 Hz, H-5), 7.10 (td, 1 H, $J_{4,6}$ 1.9 Hz, H-6), 7.38 (m, 1 H, H-7), 4.08 (dt, 1 H, J_{vic} 7.4, J_{gem} 9.4 Hz, OCH_aH_b), 3.76 (dt, 1 H, J_{vic} 7.1 Hz, OCH_aH_b), 3.05 (t, 2 H, $ArCH_2$). Anal. Calcd for $C_{15}H_{19}NO_5$ (293.32): C, 61.42; H, 6.33; N, 4.78. Found: C, 61.55; H, 6.64; N, 4.50.

The steady state NOE-difference spectra were measured using a standard pulse technique. Details have been described [37]. Longitudinal relaxation times were estimated not to exceed 2 s.

X-ray structure determination of **3**.—Crystals suitable for X-ray analysis were grown from EtOH at room temperature over three days. The crystal data and summary of the experimental details are listed in Table 6. The X-ray intensity data were collected with an Enraf–Nonius CAD4 diffractometer with nickel-filtered Cu$K\alpha$ radiation. There were no significant variations in intensity for standard reflections. The data were corrected for Lorentz and polarization effects. The

Table 7
Final atomic coordinates and equivalent isotropic thermal parameters for **3**

Atom	x	y	z	U_{eq} (Å^2)[a]
O-11	0.8979(2)	0.0184(4)	0.09236(2)	0.0593(4)
O-12	0.6135(2)	0.0940(4)	0.0824	0.0571(4)
O-13	0.7042(2)	0.3795(4)	0.04790(2)	0.0552(4)
O-14	1.0772(2)	0.4897(4)	0.03997(2)	0.0593(5)
O-15	1.0312(2)	0.1396(4)	0.05479(2)	0.0596(4)
O-16	0.7037(2)	0.3061(5)	0.11283(3)	0.0921(7)
O-18	0.5197(3)	0.2711(5)	0.01461(3)	0.0911(7)
O-20	1.0043(3)	0.6540(5)	0.01377(3)	0.0821(6)
N-1	0.5597(3)	−0.1280(6)	0.16249(4)	0.0789(7)
C-2	0.7324(3)	−0.0825(7)	0.15475(4)	0.0710(8)
C-3	0.7249(2)	−0.1994(5)	0.13658(3)	0.0537(5)
C-4	0.4335(3)	−0.4737(6)	0.11625(4)	0.0661(7)
C-5	0.2435(4)	−0.5678(8)	0.11735(5)	0.0873(10)
C-6	0.1501(3)	−0.5155(8)	0.13446(6)	0.0943(10)
C-7	0.2433(3)	−0.3706(8)	0.15061(5)	0.0840(9)
C-8	0.8841(3)	−0.1935(6)	0.12320(4)	0.0622(6)
C-9	0.8875(3)	−0.1556(6)	0.09543(4)	0.0612(6)
C-11	0.8634(3)	0.0569(5)	0.06851(3)	0.0532(5)
C-12	0.7906(2)	0.1901(5)	0.07052(3)	0.0491(5)
C-13	0.7616(2)	0.2441(5)	0.04454(3)	0.0510(5)
C-14	0.9358(3)	0.3186(6)	0.02903(3)	0.0549(6)
C-15	1.0058(3)	0.1829(6)	0.02960(3)	0.0625(6)
C-16	0.5876(3)	0.1663(6)	0.10355(3)	0.0606(6)
C-17	0.3942(3)	0.0513(8)	0.11255(5)	0.0852(9)
C-18	0.5828(3)	0.3791(6)	0.03142(4)	0.0632(7)
C-19	0.5437(5)	0.5306(8)	0.03687(5)	0.0958(10)
C-20	1.0968(3)	0.6479(6)	0.03034(4)	0.0658(7)
C-21	1.2503(4)	0.8104(9)	0.04335(5)	0.0962(13)
C-31	0.5327(2)	−0.3254(5)	0.13253(3)	0.0526(5)
C-71	0.4343(3)	−0.2766(6)	0.14923(4)	0.0637(6)

[a] $U_{eq} = (1/3)\Sigma_i\Sigma_j U_{ij} a_i^* \cdot a_j^* \mathbf{a}_i \cdot \mathbf{a}_j$.

structure was solved by the SHELX86 [38] program. Refinement was by full-matrix least-squares on F with unit weight minimising $\Sigma(|F_o| - |F_c|)^2$ with the SHELX77 [39] programme. The H atom coordinates were determined from successive difference Fourier syntheses. The H atoms attached to the terminal methyl groups (C-17, C-19, C-21) were calculated on stereochemical grounds and refined riding on their respective C atoms. Atomic scattering factors were those included in SHELX77 [39]. Details of the refinement procedure are also given in Table 6. In the structure determination of **3**, the L enantiomer was selected according to the (*S*) assignment at C-4. The molecular geometry was calculated by the program EUCLID [40]. Drawings were prepared by the program PLUTON incorporated in EUCLID [40] and ORTEP II [21]. The final atomic coordinates and equivalent isotropic thermal parameters are listed in Table 7 *.

Calculations were performed on a cluster of VAX computers, a CONVEX C-120, and on Silicon Graphics workstations at the University of Utrecht, The Netherlands, and at the X-ray Laboratory of the Ruder Bošković Institute, Zagreb, Croatia.

Acknowledgments

This work was supported by Ministry of Science and Technology grants Nos. 1-07-179 and 1-08-195, and The Commission of the European Communities, Brussels, contract No. CI1*-CT91-0891. The authors thank Dr. D. Keglević, Ruder Bošković Institute, Zagreb, for valuable comments.

References

[1] B. Kojić-Prodić, B. Nigović, S. Tomić, N. Ilić, V. Magnus, Z. Giba, R. Konjević, and W.L. Duax, *Acta Crystallogr., Sect. B*, 47 (1991) 1010–1019.
[2] B. Kojić-Prodić, B. Nigović, D. Horvatić, Ž. Ružić-Toroš, V. Magnus, W.L. Duax, J.J. Stezowski, and N. Bresciani-Pahor, *Acta Crystallogr., Sect. B*, 47 (1991) 107–115.
[3] B. Nigović, B. Kojić-Prodić, V. Puntarec, and J.D. Schagen, *Acta Crystallogr., Sect. B*, 48 (1992) 297–302.
[4] P.J. Davies, *Plant Hormones and Their Role in Plant Growth and Development*, Martinus Nijhoff, Dordrecht, 1987.
[5] V. Magnus and G. Laćan, in R.P. Pharis and S.B. Rood (Eds.), *Plant Growth Substances, Proc. 13th Int. Conf. Plant Growth Subst., Calgary, 1988*, Springer-Verlag, Berlin, Heidelberg, 1990, pp 360–366.
[6] F.W. Percival, W.K. Purves, and L.E. Vickery, *Plant Physiol.*, 51 (1973) 739–743.
[7] G. Laćan, V. Magnus, Š. Šimaga, S. Iskrić, and P.J. Hall, *Plant Physiol.*, 78 (1985) 447–454.
[8] G. Laćan, Ph.D. Thesis, University of Zagreb, Zagreb, Croatia, 1986.

* The observed and calculated structure factors, H-atom coordinates, and anisotropic thermal parameters have been deposited with the Cambridge Crystallographic Data Centre. The data may be obtained, on request, from the Director, Cambridge Crystallographic Data Centre, 12 Union Road, Cambridge, CB2 1EZ, UK.

[9] V. Magnus, *Carbohydr. Res.*, 76 (1979) 261–264.
[10] S. Jelaska, V. Magnus, M. Seretin, and G. Laćan, *Physiol. Plant.*, 64 (1985) 237–242.
[11] Cambridge Structural Database System, version 5, Cambridge Crystallographic Data Centre, Cambridge, UK, October 1992.
[12] A. Terzic, *Cryst. Struct. Commun.*, 7 (1978) 95–98.
[13] S. Aldington, G.J. McDougall, and S.C. Fry, *Plant, Cell Environ.*, 14 (1991) 625–636.
[14] H. Matsuda, Y. Ozeki, S. Amino, and A. Komamine, *Plant Cell Physiol.*, 26 (1992) 995–1001.
[15] V. Magnus, D. Vikić-Topić, S. Iskrić, and S. Kveder, *Carbohydr. Res.*, 114 (1983) 209–224.
[16] W.A. Remers, in W.L. Houlihan (Ed.), *Indoles*, Part One, Wiley, New York, 1972, pp 1–226.
[17] E.M. Arnett and C.Y. Wu, *J. Am. Chem. Soc.*, 82 (1960) 4999–5000.
[18] T.N. Sokolova, V.E. Shevchenko, and M.N. Preobrazhenskaya, *Carbohydr. Res.*, 83 (1980) 249–261.
[19] G. Alfredsson, H.B. Boren, and P.J. Garegg, *Acta Chem. Scand.*, 26 (1972) 3431–3434.
[20] A.F. Bochkov, V.I. Betanely, and N.K. Kochetkov, *Izv. Akad. Nauk SSSR, Ser. Khim.*, (1974) 1379–1386.
[21] C.K. Johnson, ORTEP II, Report ORNL-5138, Oak Ridge National Laboratory, Tennessee, USA, 1976.
[22] M. Sundaralingam, *Biopolymers*, 6 (1968) 189–213.
[23] M. Sundaralingam and L.H. Jensen, *J. Mol. Biol.*, 13 (1965) 914–929.
[24] S. Tagaki, S. Nordenson, and G.A. Jeffrey, *Acta Crystallogr., Sect. B*, 35, (1979) 991–993.
[25] D. Cremer and J.A. Pople, *J. Am. Chem. Soc.*, 97 (1975) 1354–1358.
[26] W. Klyne and V. Prelog, *Experientia*, 16 (1969) 534–568.
[27] BIOSYM, DISCOVER, version 2.7.0, Biosym Technologies (10065 Barnes Canyon Rd., San Diego, CA 92121, USA), 1991.
[28] S. Lifson and A. Warschel, *J. Chem. Phys.*, 49 (1969) 5116–5129.
[29] A.T. Hagler, Z. Huler, and S. Lifson, *J. Am. Chem. Soc.*, 96 (1974) 5319–5327.
[30] A.T. Hagler, S. Lifson, and P. Dauber, *J. Am. Chem. Soc.*, 101 (1979) 5122–5130.
[31] W.F. van Gunsteren, GROMOS, Groningen Molecular Simulation Computer Program Package, University of Groningen, The Netherlands, 1987.
[32] H.J.C. Berendsen, J.P.M. Postma, W.F. van Gunsteren, and J. Hermans, in B. Pullman (Ed.), *Intermolecular Forces*, Reidel, Dordrecht; Jerusalem Symposia, 14 (1981) 331–442.
[33] D. Neuhaus and M. Williamson, *The Nuclear Overhauser Effect in Structural and Conformational Analysis*, VCH, New York, 1989.
[34] S. Tomić, F.B. van Duijneveldt, L.M. Kroon-Batenburg, and B. Kojić-Prodić, in preparation.
[35] T.M. Kaethner, *Nature (London)*, 267 (1977) 19–23.
[36] M. Barczai-Martos and P. Körösy, *Nature (London)*, 165 (1950) 369.
[37] H. Duddeck, M. Hiegemann, M.F. Simeonov, B. Kojić-Prodić, B. Nigović, and V. Magnus, *Z. Naturforsch., Teil C*, 44 (1950) 543.
[38] G.M. Sheldrick, in G.M. Sheldrick, C. Krueger, and R. Goddard (Eds.), *Crystallographic Computing 3*, Oxford University Press, Oxford, UK, 1985.
[39] G.M. Sheldrick, SHELX77, Program for Structure Determination, University of Cambridge, Cambridge, UK, 1983.
[40] A.L. Spek, in D. Sayre (Ed.), *Computational Crystallography*, Clarendon Press, Oxford, 1982, p 528.